*Metrol. Meas. Syst.*, Vol. 30 (2023) No. 3, pp. 441–459
DOI: 10.24425/mms.2023.146423

PAN POLSKA AKADEMIA NAUK

METROLOGY AND MEASUREMENT SYSTEMS
Index 330930, ISSN 0860-8229
*www.metrology.wat.edu.pl*

M&MS

# ALGORITHMS FOR IMPROVING THE POSITION DETERMINATION OF AN UAV EQUIPPED WITH A SINGLE-FREQUENCY GPS RECEIVER FOR LOW-ALTITUDE PHOTOGRAMMETRY

**Kamil Krasuski[1)], Damian Wierzbicki[2)], Marta Lalak[1)], Adam Ciećko[3)]**

*1) Polish Air Force University, Institute of Navigation, Dywizjonu 303/35 Street, 08-521 Dęblin, Poland (k.krasuski@law.mil.pl, m.lalak@law.mil.pl)*
*2) Military University of Technology, Faculty of Civil Engineering and Geodesy, Department of Imagery Intelligence, gen. S. Kaliskiego 2 Street, 00-908 Warsaw, Poland (✉ damian.wierzbicki@wat.edu.pl)*
*3) University of Warmia and Mazury, Faculty of Geoengineering, M. Oczapowskiego 2 Street, 10-724 Olsztyn, Poland (a.ciecko@uwm.edu.pl)*

**Abstract**

The article presents the results of research on the development of a method for improving the positioning accuracy of an UAV equipped with a single-frequency GPS receiver for determining the linear elements of exterior orientation in aerial photogrammetry. Thus, the paper presents a computational strategy for improving UAV position determination using the SPP code method and the products of the IGS service. The developed algorithms were tested in two independent research experiments performed with the UAV platform on which an AsteRx-m2 UAS single-frequency receiver was installed. As a result of the experiments, it was shown that the use of IGS products in the SPP code method made it possible to improve the accuracy of the linear elements to the level of about ±2.088 m for X coordinate, ±1.547 m for Y coordinate, ±3.712 m for Z coordinate. The paper also shows the trend of changes in the obtained accuracy in determining linear elements of exterior orientation in the form of a linear regression function. Finally, the paper also applies the SBAS corrections model for the improvement of UAV position calculation and determination of linear elements of exterior orientation. In this case, the improvement in the accuracy of determining the linear elements of exterior orientation is about ±1.843 m for X coordinate, ±1.658 m for Y coordinate, ±7.930 m for Z coordinate. As the obtained test results show, the use of IGS products and SBAS corrections in the SPP code method makes it possible to improve the determination of UAV positions for the use in aerial photogrammetry.

Keywords: UAV, GNSS measurements, linear elements of exterior orientation, accuracy.

© 2023 Polish Academy of Sciences. All rights reserved

## 1. Introduction

As the technology becomes more advanced and production costs decrease, UAV platforms are becoming an increasingly interesting alternative for imaging the Earth's surface relative to the cost of implementing projects using traditional airborne imaging technologies [1]. Moreover, in

Copyright © 2023. The Author(s). This is an open-access article distributed under the terms of the Creative Commons Attribution-NonCommercial-NoDerivatives License (CC BY-NC-ND 4.0 https://creativecommons.org/licenses/by-nc-nd/4.0/), which permits use, distribution, and reproduction in any medium, provided that the article is properly cited, the use is non-commercial, and no modifications or adaptations are made.

Article history: received April 16, 2023; revised June 6, 2023; accepted June 6, 2023; available online September 20, 2023.

some cases, the use of manned aircraft for imaging may not be possible at all. In such situations, unmanned imaging platforms can be important equivalents in the implementation of imaging acquisition projects for the creation of aerial photogrammetry products [2, 3]. The use of a UAV with a mounted camera offers the possibility of acquiring high-resolution stereo images for small areas. With such data it is possible to carry out the process of digital aerotriangulation, develop a numerical terrain model, perform orthorectification and develop a digital orthophoto [4]. In the case of digital aerotriangulation, an important aspect of the process at the initial stage is the determination of approximate elements of exterior orientation [5]. To measure them, single-frequency GPS receivers [6, 7] and inertial sensors that record platform tilts are most often used [8, 9]. The approximate elements of exterior orientation are divided into linear elements representing the coordinates of the centre of projection of aerial photographs [10] and angular elements of the orientation of aerial photographs in space [11]. The coordinates of the centre of the projection of aerial photos were assumed to be denoted as $(X_o, Y_o, Z_o)$, and the angular coordinates of the orientation of the camera as $(H, P, R)$ [12]. For the purpose of determining the coordinates of the centre of projection of aerial photographs, it is necessary to know the excentre of the position offset of the GPS receiver antenna and camera at the time of exposure [13]. While the value of the excentre is provided in the UAV platform specific metric by the manufacturer, the position of the GPS receiver antenna mounted on the platform must be determined. Low-cost UAVs are equipped with single-frequency GPS receivers to record GPS code observations to determine UAV coordinates [14]. Based on the recording of GPS code observations, it is possible to determine the UAV's position by using the *Single Point Positioning* (SPP) absolute positioning method [15]. The problem of the SPP code method for UAV positioning is its low positioning accuracy, reaching down to 10 m [16]. The low positioning accuracy of the UAV ultimately results in low accuracy in determining the approximate linear elements of the exterior orientation. Therefore, it is necessary to develop numerical algorithms to improve the accuracy of SPP code positioning for the UAV platform. For the SPP code method, *Satellite-based Augmentation Systems* (SBAS) corrections [17] and *International GNSS Service* (IGS) geodetic service products [18] can be applied to improve the determination of UAV position accuracy and approximate linear elements of exterior orientation.

## 2. Literature review

Up to now, as shown by the analysis of the state of the art, the topic of UAV platform positioning using GPS satellite technology has been presented in many research works. Thus, in the case of GPS positioning, one of the key elements is the development of algorithms for controlling and monitoring changes in the platform's coordinates in relation to the reference flight trajectory [19]. This is important because the development of appropriate algorithms for monitoring the flight of a UAV allows to avoid collisions in space and safely transport various types of goods and services [20]. The developed algorithms for determining UAV coordinates can be based on the concept of GPS/INS (*inertial navigation system*) positioning using Kalman filtering [21]. UAV positioning typically uses single-frequency GPS receivers with different accuracy classes under the SPP code positioning method [22, 23]. This, in turn, affects the accuracy of real-time UAV position determination during the execution of photogrammetric raids [24]. The accuracy of GPS single-frequency positioning for UAVs in real time can be improved using SBAS augmentation systems [25, 26]. On this basis, it is possible to determine the reliability of UAV positioning in accordance with ICAO requirements [27]. How important the accuracy and integrity of UAV positioning is can be seen in the works [28–30], where the

*Metrol. Meas. Syst.*, Vol. 30 (2023), No. 3, pp. 441–459
DOI: 10.24425/mms.2023.146423

effects of intentional spoofing the determination of UAV position using GPS navigation systems is shown. As regards UAV positioning using GPS single-frequency receivers, it is also possible to monitor the status of the ionosphere [31] or also air pollution in the troposphere [32]. GPS single-frequency positioning has its direct impact on photogrammetric and remote sensing applications in UAV technology. The following research developments can be mentioned for these applications: the impact of GPS single-frequency positioning quality on the development of map products in professional photogrammetry [33], detection and localization of moving objects in aerial photographs taken from low altitude by UAVs [34], determination of exterior orientation elements in the process of digital aerotriangulation based on the use of data from a single-frequency GPS receiver mounted on a UAV [35], determination of approximate accuracy of control points for photogrammetric applications [36–38], detection and localization of a standing object in aerial photographs taken from low altitude by a UAV [39], analysis of the accuracy of the digital aerotriangulation process for alignment of a block of aerial photographs taken by a UAV [40,41], application of UAV technology in navigation in heavily and poorly urbanized areas [42], UAV positioning improvements for GPS/RADAR solution [43] and GPS/INS/LiDAR [44].

The following conclusions can be drawn from the analysis of the state of the art: low accuracy of GPS single-frequency positioning for UAV technology for typical navigation purposes can be noted; the obtained low accuracy of GPS single-frequency positioning for UAV technology translates into the quality of final photogrammetric products in the aerotriangulation process; single-frequency GPS positioning for UAV technology applied the SPP code method to determine the coordinates of the unmanned platform; attempts to improve UAV position determination were based on the application of SBAS corrections in the observation algorithm or the use of Kalman filtering as a method for determining UAV position.

On this basis, the missing elements in the state-of-the-art analysis can be identified. Firstly, it is necessary to optimize the UAV position calculation process with a selected measurement strategy. This is mainly about the possibility of using IGS products and *European Geostationary Navigation Overlay Service* (EGNOS) corrections in the process of developing GPS code observations. Thus, some systematic error models in the observation equation of the SPP code method will be changed. In this sense, the orbit errors, satellite clock biases, ionosphere and troposphere errors could be reduced. Especially, the GPS satellite positions were calculated using the Lagrange polynomial model based on IGS products and using EGNOS long time corrections in SBAS solutions. Next, GPS satellite clock bias was estimated using the Lagrange polynomial model based on IGS products and using EGNOS long time corrections in the SBAS solution. In turn, the ionosphere delay was determined based on the IONEX format as an IGS product and using the EGNOS ionospheric model in the SBAS solution. Moreover, the troposphere delay could be reduced using the SNX_TRO format as an IGS product and using the *Radio Technical Commission for Aeronautic – Minimum Operational Performance Standards* (RTCA-MOPS) model in the SBAS solution.

Secondly, it seems worth determining how the use of IGS products and EGNOS corrections affects the determination of UAV positions and calculation of approximate line elements of exterior orientation. It means how IGS products and EGNOS corrections improved the accuracy terms of an UAV position in relation to the standalone GPS solution. In addition, how IGS products and EGNOS corrections improved the linear elements of exterior orientation in photogrammetry application.

Finally, it is necessary to determine the trend of changes for the calculated results of accuracy of the approximate linear elements of exterior orientation during the photogrammetric flight. It is important in detection of blunder errors in the linear elements of the external orientation. Moreover, the direction of the trend of change shows whether linear elements of the external orientation are increasing or decreasing for a series of images.

## 3. Research methods

This section describes and presents the basic observation equations for the SPP code positioning method for UAV technology. For this purpose, the following algorithms are presented:

- the solution of the classical SPP using only GPS code observations and a GPS navigation message (method No. 1),
- the solution of SPP using GPS code observations and IGS products (method No. 2),
- the solution of SPP using GPS code observations and EGNOS corrections (method No. 3).

Research methods No. 2 and 3 are designed to improve the determination of UAV position coordinates, and thus improve the accuracy of UAV positioning relative to the classical solution used in method No. 1.

The basic observation equation for SPP positioning method No. 1 takes the form as written below [45]:

$$l = d + c \cdot (dtr - dts) + Ion + Trop + Rel + \mathrm{TGD}, \tag{1}$$

where: $l$ – pseudorange (code measurement) on L1 frequency in the GPS system; $d$ – geometric distance between the satellite and the receiver, taking into account the correction of the Sagnac effect; $d = \sqrt{(X - X_{\mathrm{GPS}})^2 + (Y - Y_{\mathrm{GPS}})^2 + (Z - Z_{\mathrm{GPS}})^2}$; $(X, Y, Z)$ – UAV coordinates, parameters determined in the process of developing GPS code observations; $(X_{\mathrm{GPS}}, Y_{\mathrm{GPS}}, Z_{\mathrm{GPS}})$ – GPS satellite coordinates in the XYZ geocentric system, the coordinates are determined from the Kepler orbit model; $c$ – speed of light; $dtr$ – receiver clock correction, a parameter determined together with the UAV coordinates; $dts$ – the satellite clock correction, determined from the 2$^{\mathrm{nd}}$ degree polynomial from the GPS navigation message; $Ion$ – ionospheric correction, in the SPP method determined based on the Klobuchar model; $Trop$ – tropospheric correction, determined based on a deterministic model of tropospheric delay; $Rel$ – relativistic effect, determined from navigation message data; TGD – the Timing Group Delay determined on the basis of data from the navigation message.

In turn, the basic observation equation for the No. 2 SPP positioning method takes the following form [46, 47]:

$$l = d' + c \cdot (dtr - dts') + Ion' + Trop + Rel + \mathrm{SDCB}'_{P1} + \mathrm{RDCB}'_{P1}, \tag{2}$$

where: $l$ – pseudorange (code measurement) on L1 frequency in GPS system; $d'$ –geometric distance between the satellite and the receiver, taking into account the correction of the Sagnac effect and the phase centre characteristics of the satellite and receiver antennas based on the ANTEX format; $d' = \sqrt{(X - X'_{\mathrm{GPS}})^2 + (Y - Y'_{\mathrm{GPS}})^2 + (Z - Z'_{\mathrm{GPS}})^2}$; $(X, Y, Z)$ – UAV coordinates, parameters determined using IGS products; $(X'_{\mathrm{GPS}}, Y'_{\mathrm{GPS}}, Z'_{\mathrm{GPS}})$ – GPS satellite coordinates in the XYZ geocentric frame, the coordinates are determined from the Lagrange polynomial based on the EPH precise ephemeris from the IGS service; $c$ – speed of light; $dtr$ – receiver clock correction, a parameter determined together with the UAV coordinates; $dts'$ – the satellite clock correction, determined using the CLK format from the IGS service; $Ion'$ – ionospheric correction, is interpolated using the GRID from the IONEX format of the IGS service; $Trop$ – tropospheric correction, determined based on a deterministic model of tropospheric delay or using the SNX_TRO format from the IGS service; $Rel$ – relativistic effect, determined from EPH precise ephemeris data; $\mathrm{SDCB}'_{P1}$ – hardware delay for $\mathrm{SDCB}_{P1}$ satellite, based on the DCB product from IGS service; $\mathrm{RDCB}'_{P1}$ – hardware delay for $\mathrm{RDCB}_{P1}$ receiver, determined with a Geometry-Free linear combination or based on the DCB product from IGS service.

*Metrol. Meas. Syst.*, Vol. 30 (2023), No. 3, pp. 441–459
DOI: 10.24425/mms.2023.146423

Finally, the basic observation equation for SPP positioning with SBAS/EGNOS corrections takes the following form [48, 49]:

$$l = d^* + c \cdot (dtr - dts^*) + Ion^* + Trop^* + Rel + \mathrm{TGD} + \mathrm{FC}, \tag{3}$$

where: $l$ – pseudorange (code measurement) on L1 frequency in GPS system; $d^*$ – geometric distance between the satellite and the receiver, taking into account the correction of the Sagnac effect and long term SBAS corrections; $d^* = \sqrt{(X - X^*_{\mathrm{GPS}})^2 + (Y - Y^*_{\mathrm{GPS}})^2 + (Z - Z^*_{\mathrm{GPS}})^2}$; $(X, Y, Z)$ – UAV coordinates, parameters determined in the process of developing GPS code observations; $(X^*_{\mathrm{GPS}}, Y^*_{\mathrm{GPS}}, Z^*_{\mathrm{GPS}})$ – GPS satellite coordinates in the XYZ geocentric system, the coordinates are determined from the Kepler orbit model, taking into account long term SBAS corrections; $c$ – speed of light; $dtr$ – receiver clock correction, a parameter determined together with the UAV coordinates; $dts^*$ – the satellite clock correction, determined from the 2$^{\mathrm{nd}}$ degree polynomial from the GPS navigation message, taking into account long term SBAS corrections; $Ion^*$ – ionospheric correction, determined using the SBAS ionosphere model; $Trop^*$ – tropospheric correction, determined from the RTCA-MOPS model dedicated to SBAS augmentation systems; $Rel$ – relativistic effect, determined from navigation message data; TGD – the Timing Group Delay determined on the basis of data from the GPS navigation message, FC – fast SBAS corrections.

Using this method, the accuracy of the determination of the approximate linear elements of the exterior orientation will be calculated as shown below [12, 50]:

$$\begin{cases} \mathrm{d}X = X_o - X_{\mathrm{ref},o} \\ \mathrm{d}Y = Y_o - Y_{\mathrm{ref},o} \\ \mathrm{d}Z = Z_o - Z_{\mathrm{ref},o} \end{cases}, \tag{4}$$

where: $(X_{\mathrm{ref}}, Y_{\mathrm{ref}}, Z_{\mathrm{ref}})$ – reference values of the linear elements of the exterior orientation, determined in the post-processing mode; $X_{\mathrm{ref},o} = X_{\mathrm{ref}} + e_X$; $X_{\mathrm{ref}}$ – reference trajectory of the UAV flight along the X axis, determined using the RTK technique; $Y_{\mathrm{ref},o} = Y_{\mathrm{ref}} + e_Y$; $Y_{\mathrm{ref}}$ – reference trajectory of the UAV flight along the Y axis, determined using the RTK technique; $Z_{\mathrm{ref},o} = Z_{\mathrm{ref}} + e_Z$; $Z_{\mathrm{ref}}$ – reference trajectory of the UAV flight along the Z axis, determined using the RTK technique.

The presented mathematical algorithm (1–4) defines a computational strategy based on the application of the observation equation for the SPP code method to determine the approximate linear elements of the exterior orientation. However, it is also possible to additionally apply mathematical functions that determine the trend of change for the determined parameters ($\mathrm{d}X\mathrm{d}Y\mathrm{d}Z$). For this purpose, a mathematical function in the form of a polynomial of degree 1 model was used. The polynomial of degree 1 model commonly referred to as linear regression can be described for the parameters ($\mathrm{d}X\mathrm{d}Y\mathrm{d}Z$) as [51]:

$$\mathrm{d}X = a_X \cdot t + b_X\,, \tag{5}$$

$$\mathrm{d}Y = a_Y \cdot t + b_Y\,, \tag{6}$$

$$\mathrm{d}Z = a_Z \cdot t + b_Z\,, \tag{7}$$

where: $t$ – measurement epoch, time of observation; $(a_X, b_x)$ – determined linear coefficients of the polynomial of degree 1 for the parameter $\mathrm{d}X$; $(a_Y, b_Y)$ – determined linear coefficients of the polynomial of degree 1 for the parameter $\mathrm{d}Y$; $(a_Z, b_Z)$ – determined linear coefficients of the polynomial of degree 1 for the parameter $\mathrm{d}Z$.

The mathematical equations (5)–(7), assuming that the number of the input set of given parameters ($\mathrm{d}X\mathrm{d}Y\mathrm{d}Z$) is much larger than the number of coefficients to be determined are solved

with the least squares method as follows [52]:

$$\begin{cases} Qx = N^1 \cdot L \\ v = A \cdot Qx - dl \\ m0 = \sqrt{\dfrac{[vv]}{r-s}} \end{cases}, \tag{8}$$

where: $Qx$ – vector with the determined linear coefficients of the polynomial (2 coefficients each for the parameters $\mathrm{d}X\mathrm{d}Y\mathrm{d}Z$); $N = A^T \cdot A$ – system of normal equations; $A$ – coefficient matrix; $L = A^T \cdot dl$; $dl$ – vector with difference between measurements and modeled parameters; $m$ – standard deviation of corrections; $r$ – number of observations of the input set, $r > 2$ for mathematical equations (5–7); $s$ – number of coefficients to be determined, $s = 2$ for mathematical equations (5–7); $v$ – correction vector.

## 4. Research experiment

As part of the research test, a test flight was performed using a UAV platform on which an AsteRx-m2 UAS single-frequency receiver was installed to log GPS observations and navigation data. The test flight was conducted on 7 September 2020 in the first test area, in northern Poland, from 09:58:19 to 10:13:11 according to GPST. The flight height was between 100 and 130 m. The air temperature during the flight was 17°C and the wind speed was 4.5 m/s. The flight scenario had been planned so that the mission coverage did not include an urban area. The flight was conducted in an east-west direction. The purpose of the test flight carried out was to verify and test the performance of the proposed test methods for equations (1)–(2) and the algorithms from equations (5)–(7). In addition, several hundred images were acquired as part of the survey campaign for the realisation of photogrammetric studies, the longitudinal and transverse coverage of the images was 75%. Based on the algorithms for research methods No. 1–2, the UAV coordinates were determined, followed by the linear elements of the exterior orientation. For research method No. 1, GPS observations and navigation data were used. For research method No. 2, GPS observations and IGS geodetic products were used in the form of EPH precision ephemeris, CLK precision clock format, satellite/receiver antenna phase centre characteristics from the ANTEX format, global ionosphere maps from the IONEX format and hardware delays from the DCB format [53]. Mathematical calculations for equations (1)–(2) were performed in RTKLIB v.2.4.2 [54]. Next, the determination of the UAV's precise flight trajectory was performed using the differential phase technique RTK [55]. The calculations at this stage were performed in Topcon MAGNET Tools v.5.1.1.0 [56]. Next, the mathematical algorithm (4) for calculating the approximate linear elements of the exterior orientation were implemented into a numerical script developed in the Scilab v.6.0.0 language environment [57]. At this stage, the obtained parameter results ($\mathrm{d}X\mathrm{d}Y\mathrm{d}Z$) were subjected to a smoothing process using the equation models (5–7). In addition, the coefficients from equation (8) and the statistical parameters were determined according to equation (8), *i.e.*, the distribution of the corrections and the standard deviation. The final results derived from the mathematical equations (4)–(8) were presented graphically using Scilab.

## 5. Research results

As part of the analysis of the test results obtained, the values of the parameters ($\mathrm{d}X\mathrm{d}Y\mathrm{d}Z$) calculated from equation (4) are shown first. Figures 1–3 show the results of the accuracy of the determination of the approximate linear elements of the exterior orientation. The results of the

*Metrol. Meas. Syst.*, Vol. 30 (2023), No. 3, pp. 441–459
DOI: 10.24425/mms.2023.146423

parameters (d$X$d$Y$d$Z$) calculated from the comparison of the classical SPP solution against the differential RTK solution (blue) and the comparison of the SPP solution with the IGS products against the differential RTK solution (red) are juxtaposed. The accuracy of the determination of the exterior orientation elements along the X-axis using test method No. 1 ranges from −2.899 m to +2.796 m. In contrast, for test method No. 2, the accuracy of d$X$ is +0.123 m to +2.088 m. The use of IGS products in test method No. 2 enabled an improvement in the accuracy of the determination of the exterior orientation elements along the X-axis by 44% relative to the SPP solution using test method No. 1.

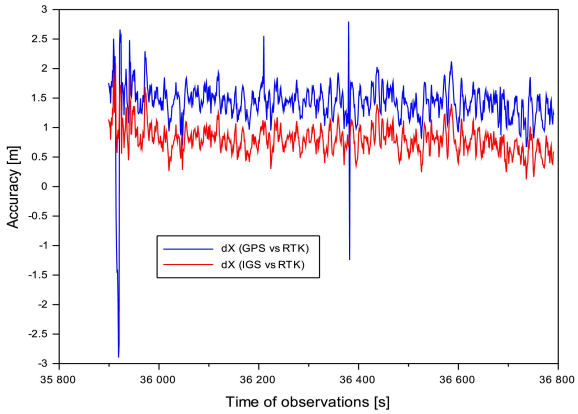


Fig. 1. Accuracy of linear elements of exterior orientation along the X-axis in the 1st flight test.

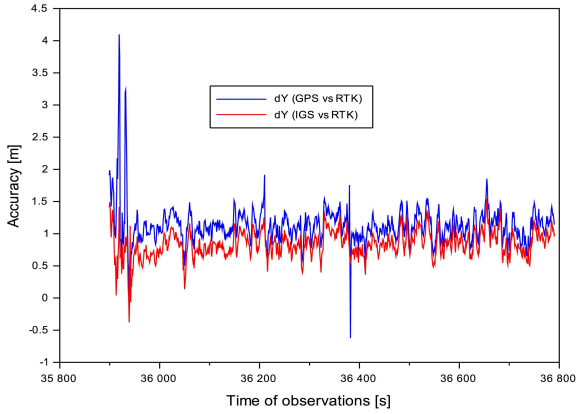


Fig. 2. Accuracy of linear elements of exterior orientation along the Y-axis in the 1st flight test.

The accuracy of the determination of the elements of the exterior orientation along the Y-axis using test method No. 1 ranges from −0.622 m to +4.099 m. In contrast, for test method No. 2, the accuracy of d$Y$ is −0.377 m to +1.547 m. The use of IGS products in test method No. 2 enabled an improvement in the accuracy of the determination of the exterior orientation elements along the Y-axis by 26% relative to the SPP solution using test method No. 1.

The accuracy of the determination of the exterior orientation elements along the Z-axis for test method No. 1 ranges from −7.585 m to +4.017 m. In contrast, for test method No. 2, the

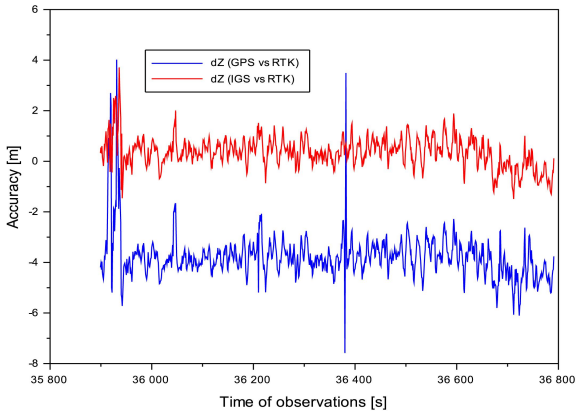


Fig. 3. Accuracy of linear elements of exterior orientation along the Z-axis in the 1st flight test.

accuracy of d$Z$ is −1.491 m to +3.712 m. The use of IGS products in test method No. 2 enabled the accuracy of the determination of external orientation elements along the Z-axis to be improved by 90% relative to the SPP solution using test Method No. 1.

In order to determine the trend of change for the parameters (d$X$d$Y$d$Z$), a 1-degree polynomial model was used in the subsequent numerical accuracy analysis using equations (5)–(8). Fig. 4 shows the results of the time-variation characteristics for the parameter d$X$. The trend of change of the d$X$ parameter for method No. 1 can be described by a linear regression function as: $\mathrm{d}X = -0.0001491 \cdot t + 1.4837426$. The scatter of the $v$-corrections for this function ranges from −1.384 m to +4.379 m. The standard deviation parameter of the corrections – $m$ is 0.396 m and determines in this case the fit of the d$X$ results with respect to the linear regression. In contrast, the trend of the changes of the parameter d$X$ for method No. 2 can be described by the linear regression function as: $\mathrm{d}X = -0.0003279 \cdot t + 0.9444870$. Furthermore, the scatter of the $v$-corrections for this function ranges from −1.149 m to +0.640 m. In contrast, the standard deviation of the corrections – $m$ is 0.221 m in this case. For a better description of the linear regression, the $R^2$ determination coefficient was estimated [58]. In this case, the $R^2$ determination coefficient amounts to 0.75 for methods No. 1 and No. 2.

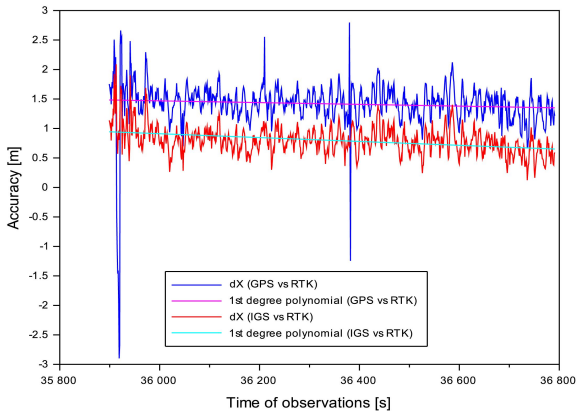


Fig. 4. Trend of changes of the parameter d$X$ in the 1st flight test.

*Metrol. Meas. Syst.*, Vol. 30 (2023), No. 3, pp. 441–459
DOI: 10.24425/mms.2023.146423

Figure 5 shows the trend of change of the parameter d$Y$ using a 1-degree polynomial. The trend of change of the parameter d$Y$ for method No. 1 can be described by a linear regression function as: $dY = -0.0001023 \cdot t + 1.17620$. The scatter of the $v$-corrections for this function is −2.925 m to +1.749 m. The standard deviation parameter of the corrections – $m$ is equal to 0.296 m. In contrast, the trend in changes of the parameter d$Y$ for method No. 2 can be described by a linear regression function as: $dY = 0.0002147 \cdot t + 0.7451850$. In addition, the scatter of the $v$-corrections for this function is from −0.742 m to +1.131 m. In contrast, the standard deviation of the corrections – $m$ is 0.201 m in this case. For parameter d$Y$, the $R^2$ determination coefficient equals 0.75 for methods No. 1 and No. 2.

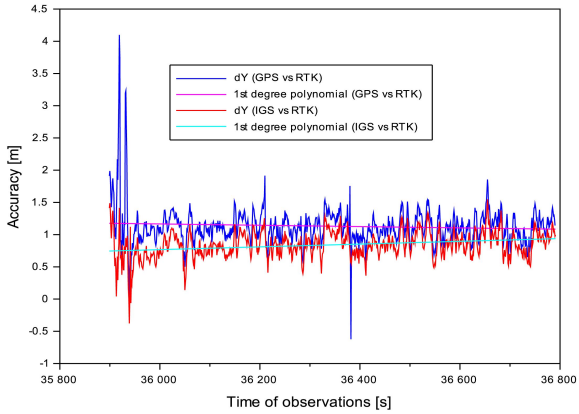


Fig. 5. Trend of changes of the parameter d$Y$ in the 1st flight test.

Figure 6 shows the trend of change of the parameter d$Z$ using a 1-degree polynomial. The trend of change of the parameter d$Z$ for method No. 1 can be described by a linear regression function as: $dZ = -0.0008593 \cdot t - 3.3938353$. The scatter of the $v$-corrections for this function is from −7.439 m to +3.776 m. The standard deviation parameter of the corrections – $m$ is equal to 0.879 m. In contrast, the trend of change in the parameter d$Z$ for method 2 can be described by a linear regression function as: $dZ = -0.0007064 \cdot t + 0.6696555$. In addition, the scatter of

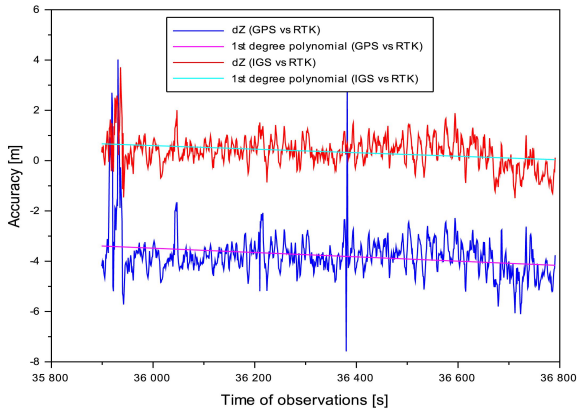


Fig. 6. Trend of changes of the parameter d$Z$ in the 1st flight test.

the $v$-corrections for this function ranges from −3.069 m to +2.099 m. In contrast, the standard deviation of the corrections – $m$ is 0.565 m in this case. For parameter d$Z$, the $R^2$ determination coefficient equals 0.75 for methods No. 1 and No. 2.

## 6. Discussion

The discussion covers three main topics, *i.e.*, the reproducibility of the computational process, the use of an alternative method to improve determining the UAV's position, and the comparison of the obtained research results in relation to the state-of-the-art analysis.

### *6.1. The reproducibility of the proposed computational process*

The developed algorithms were tested and proven in photogrammetric application in another flight of the UAV platform. This time, the flight took place in the second test area in northern Poland on 07.09.2020 from 11:59:01 to 12:10:45 according to GPST time. The air temperature during the flight was 18°C and the wind speed was 3 m/s. The flight height was 150 m. Again, the flight scenario had been planned so that the mission coverage was not over an urban area. The flight was conducted in an east-west direction. As part of the flight, several hundred images were also taken for the realisation of photogrammetric studies, the longitudinal and transverse coverage of the images was 75%.

Figures 7–9 present the results of the accuracy of the exterior orientation elements determination along the XYZ-axes using test method No. 1 and No. 2. They also show the results of the time variation of the parameters (d$X$, d$Y$, d$Z$). The accuracy of the determination of the elements of exterior orientation along the X axis using test method No. 1 ranges from −0.224 m to +3.350 m. In contrast, for test method No. 2, the accuracy of d$X$ is −0.792 m to +2.273 m. The use of IGS products in test method No. 2 enabled the accuracy of the determination of the exterior orientation elements along the X-axis to be improved by approximately 45% relative to the SPP solution using test method No. 1. The trend of change in the parameter d$X$ for test method No. 1 can be described by a linear regression function as: $\mathrm{d}X = -0.0006215 \cdot t + 0.9778952$. The scatter of the $v$-corrections for this function ranges from −2.381 m to +0.930 m. The standard deviation parameter of the corrections – $m$ is 0.285 m. In contrast, the trend of change in the parameter d$X$ for method No. 2 can be described by a linear regression function as:

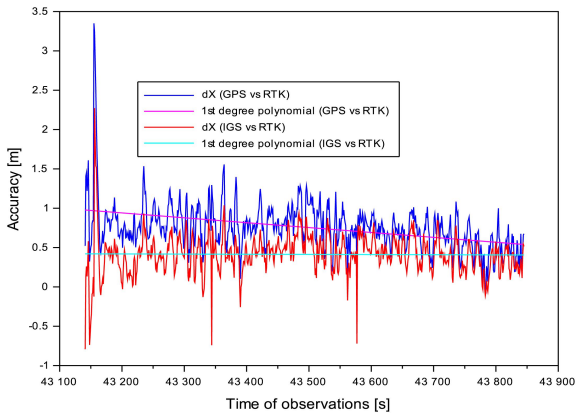


Fig. 7. Trend of changes of the parameter d$X$ in the 2nd flight test.

*Metrol. Meas. Syst.*, Vol. 30 (2023), No. 3, pp. 441–459
DOI: 10.24425/mms.2023.146423

$dX = -0.0000202 \cdot t + 0.4203586$. In addition, the scatter of the $v$-corrections for this function ranges from −1.853 m to +1.212 m. In contrast, the standard deviation of the corrections – $m$ is 0.254 m in this case. For parameter $dX$, the $R^2$ determination coefficient equals 0.75 for methods No. 1 and No. 2.

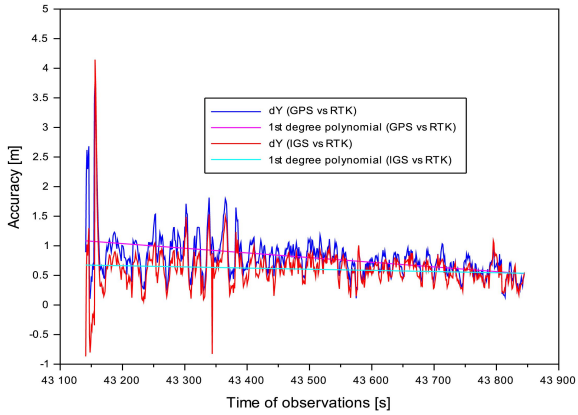


Fig. 8. Trend of changes of the parameter $dY$ in the 2nd flight test.

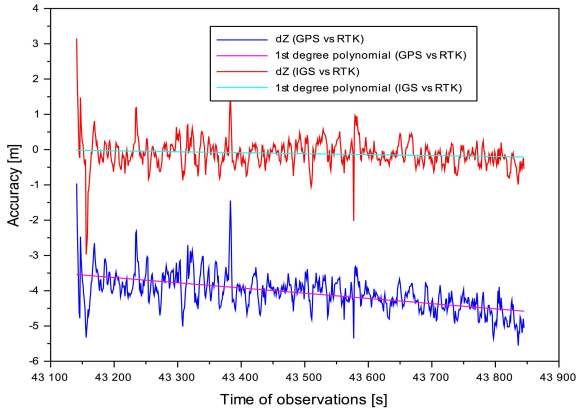


Fig. 9. Trend of changes of $dZ$ parameter in the 2nd flight test.

The accuracy of the determination of the elements of exterior orientation along the Y-axis using test method No. 1 ranges from +0.105 m to +3.790 m. In contrast, for test method No. 2, the accuracy of $dY$ is −0.867 m to +4.145 m. The use of IGS products in test method No. 2 enabled the accuracy of the determination of the exterior orientation elements along the Y-axis to be improved by approximately 25% relative to the SPP solution using test method No. 1. The trend of change in the parameter $dY$ for method No. 1 can be described by a linear regression function as: $dY = -0.000788 \cdot t + 1.0845907$. The scatter of the $v$-corrections for this function ranges from −2.718 m to +0.973 m. The standard deviation parameter of the corrections – $m$ is 0.335 m. In contrast, the trend of change in the parameter $dY$ for method No. 2 can be described by a linear regression function as: $dY = -0.0001968 \cdot t + 0.6749552$. In addition, the scatter of

the $v$-corrections for this function is between −3.473 m and +1.542 m. In contrast, the standard deviation parameter of the corrections – $m$ is 0.323 m in this case. For parameter d$Y$, the $R^2$ determination coefficient is close to 0.75 for methods No. 1 and No. 2.

The accuracy of the determination of the elements of exterior orientation along the Z-axis using test method No. 1 ranges from −5.556 m to −0.962 m. In contrast, for test method No. 2, the accuracy of d$Z$ is −2.970 m to +3.146 m. The use of IGS products in test method No. 2 enabled the accuracy of the determination of the exterior orientation elements along the Z-axis to be improved by approximately 97% relative to the SPP solution using test method No. 1. The trend of change in the parameter d$Z$ for test method No. 1 can be described by a linear regression function as: $dZ = -0.0014775 \cdot t - 3.5390173$. The scatter of the $v$-corrections for this function ranges from −2.578 m to +1.765 m. The standard deviation parameter of the corrections – $m$ is 0.424 m. In contrast, the trend in change of the parameter d$Z$ for method No. 2 can be described by a linear regression function as: $dZ = -0.0002709 \cdot t - 0.0177996$. In addition, the scatter of the $v$-corrections for this function is from −3.164 m to +2.948 m. In contrast, the standard deviation parameter of the corrections – $m$ is 0.415 m in this case. For parameter d$Z$, the $R^2$ determination coefficient amounts to 0.75 for methods No. 1 and No. 2.

### *6.2. Use of SBAS/EGNOS corrections as an alternative method to improve UAV position determination*

In the second part of the discussion, an alternative algorithm is presented to improve the determination of the UAV's position and thus improve the accuracy of the determination of the linear elements of the exterior orientation. Namely, for this purpose, SBAS corrections from the EGNOS augmentation system [59] were applied to modify the observation equation in the SPP code method. Equation (3) is used to improve the SPP code positioning with SBAS corrections and, for the purpose of the present study, defines test method No. 3. From equation (3), the XYZ geocentric coordinates of the UAV position are determined, and then the approximate linear elements of the external orientation are calculated according to equation (4). Subsequently, the accuracy parameters (d$X$d$Y$d$Z$) are determined according to equation (4). Figures 10–12 compare the parameters (d$X$d$Y$d$Z$) determined from test method No. 1 and 3. Test data from the first test area of flight No. 1 were used in the comparative analysis. The accuracy of determination of the parameters (d$X$d$Y$d$Z$) using test method No. 1 is discussed and presented in Section 5 of

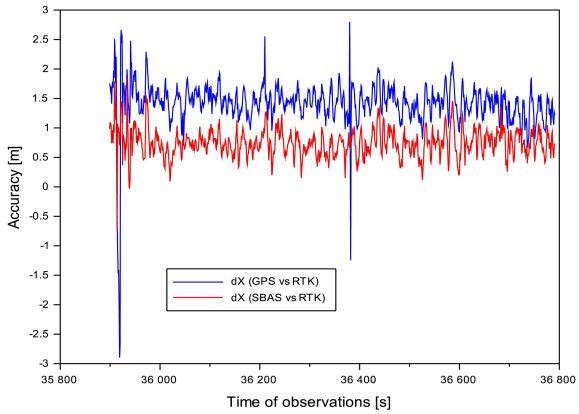


Fig. 10. Accuracy of linear elements of exterior orientation along the X-axis in the 2nd flight test.

*Metrol. Meas. Syst.*, Vol. 30 (2023), No. 3, pp. 441–459
DOI: 10.24425/mms.2023.146423

this paper. On the other hand, the accuracy of the determination of the parameters ($dXdYdZ$) using test method No. 3 ranges from −0.755 m to +1.843 m along the X axis, from −0.499 m to +1.658 m along the Y axis, from −2.126 m to +7.930 m along the Z axis, respectively. And further, the application of EGNOS corrections in the SPP code method allowed to increase the accuracy of the determination of the linear elements of the exterior orientation by respectively: 48% along the X-axis, 38% along the Y-axis and 77% along the Z-axis relative to the results obtained for test method No. 1.

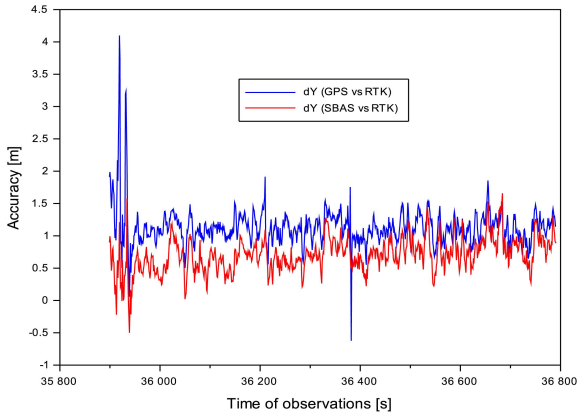


Fig. 11. Accuracy of linear elements of exterior orientation along the Y-axis in the 2nd flight test.

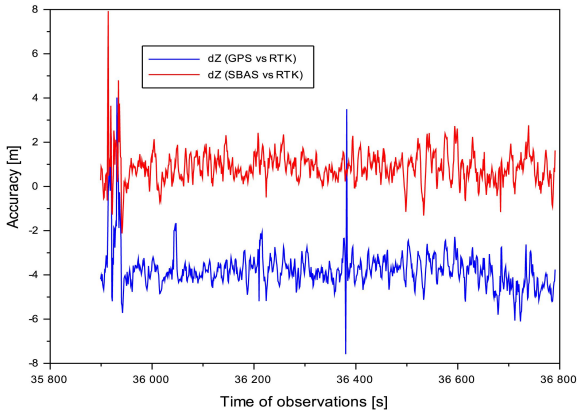


Fig. 12. Accuracy of linear elements of exterior orientation along the Z-axis in the 2nd flight test.

Similarly to method No. 2, the use of method No. 3 to improve the determination of UAV coordinates and at the same time improve the accuracy of the determination of the linear elements of the exterior orientation is reasonable in practice. As the test results show, test methods No. 2 and 3 have proven to be effective in photogrammetric applications. This is particularly relevant when using single-frequency GPS receivers and code-based positioning algorithms for UAV technology. A summary comparison of the obtained accuracy results of the linear elements of the exterior orientation in flight test in the first test area is shown in Table 1.

Table 1. Comparison of accuracy of linear elements of exterior orientation based on three research methods

| Accuracy parameter | Method No. 1 | Method No. 2 | Method No. 3 |
|---|---|---|---|
| d$X$ | −2.899 m to +2.796 m | +0.123 m to +2.088 m | −0.755 m to +1.843 m |
| d$Y$ | −0.622 m to +4.099 m | −0.377 m to +1.547 m | −0.499 m to +1.658 m |
| d$Z$ | −7.585 m to +4.017 m | −1.491 m to +3.712 m | −2.126 m to +7.930 m |

### *6.3. Comparison of research results obtained with reference to the state-of-the-art analysis*

The third part of the discussion compares the obtained research results in the context of the current state of knowledge. Based on the results, it can be concluded that:

- the use of IGS products in the SPP code method improved the UAV positioning accuracy quite significantly, similarly to the work [46],
- the use of SBAS corrections in the SPP code method improved UAV positioning accuracy quite significantly, similarly to the studies [25, 26],
- the accuracy of the determination of the approximate elements of the exterior orientation was determined in this work, similarly to the works [12],
- the obtained final UAV positioning accuracy due to IGS products and SBAS corrections is higher than the accuracy results shown in papers [24, 25],
- the algorithms developed in this work could potentially be used in the studies [27, 31, 33–35, 39, 43, 44].

## 7. Conclusions

This article presents the results of experimental research and numerical analysis of UAV position determination and determination of linear elements of exterior orientation for aerial photogrammetry. The main objective of the research was to develop a methodology to improve the accuracy of determining the linear elements of exterior orientation by using algorithms to improve the position determination of a UAV equipped with a single-frequency GPS receiver. For this purpose, the SPP code method algorithm modified with IGS service products, *i.e.*, EPH precision ephemeris, CLK precision clocks, the IONEX format, the DCB format, the ANTEX format, was used. The developed algorithm was tested in two independent research experiments performed with the UAV platform, on which an AsteRx-m2 UAS single-frequency receiver was installed. Based on the analysis, it was found that the use of the SPP absolute positioning method algorithm with IGS products improved the determination of the UAV's position and improved the accuracy of determining the linear elements of the exterior orientation. The use of IGS products in the SPP code method made it possible to improve the accuracy of determining the linear elements of exterior orientation to the level of about ±2.088 m for X coordinate, ±1.547 m for Y coordinate, ±3.712 m for Z coordinate. For the obtained results of the accuracy of determination of linear elements of exterior orientation, trends of changes as a function of time were determined in the form of a linear regression function. The paper also applied an alternative algorithm for improving the determination of UAV positions and linear elements of exterior orientation based on the use of SBAS corrections. In this case, the improvement in the accuracy of determining the linear elements of exterior orientation is about ±1.843 m for X coordinate, ±1.658 m for Y coordinate, ±7.930 m for Z coordinate. Based on the results obtained, it can be said that the use of IGS products and SBAS corrections in the SPP code method makes it possible to improve

*Metrol. Meas. Syst.*, Vol. 30 (2023), No. 3, pp. 441–459
DOI: 10.24425/mms.2023.146423

the position determination of a UAV equipped with a single-frequency GPS receiver for use in photogrammetry. In addition, the presented research methods could be used:

- in aerial navigation for flight planning and flight trajectory correction in real time,
- in geodesy for reduction and modelling the systematic biases in GPS observations,
- in aerial transport for determination the accuracy parameter as one of factors of quality of GPS satellite positioning,
- in aerial photogrammetry for approximate orientation the block images,
- in aerial photogrammetry in the initial phase of aerotriangulation processing.

## Acknowledgements

This research was supported by the Military University of Technology, Faculty of Civil Engineering and Geodesy and the Polish Air Force University, Institute of Navigation in the year 2023.

## References

[1] Udin, W. S., & Ahmad, A. (2014, February). Assessment of photogrammetric mapping accuracy based on variation flying altitude using unmanned aerial vehicle. In *IOP conference series: earth and environmental science* (Vol. 18, No. 1, p. 012027). IOP Publishing. https://doi.org/10.1088/1755-1315/18/1/012027

[2] Elkhrachy, I. (2021). Accuracy assessment of low-cost unmanned aerial vehicle (UAV) photogrammetry. *Alexandria Engineering Journal*, 60(6), 5579–5590. https://doi.org/10.1016/j.aej.2021.04.011

[3] Sung, H., Chong, K., & Lee, C. N. (2019). Accuracy analysis of low-cost UAV photogrammetry for road sign positioning. *Journal of the Korean Society of Surveying, Geodesy, Photogrammetry and Cartography*, *37*(4), 243–251. https://doi.org/10.7848/ksgpc.2018.36.6.565

[4] Wierzbicki, D., Kędzierski, M., & Fryskowska, A. (August, 2015). Assessment of the influence of UAV image quality on the orthophoto production. In *Proceedings of the International Archives of the Photogrammetry, Remote Sensing and Spatial Information Sciences*, Canada. https://doi.org/10.5194/isprsarchives-XL-1-W4-1-2015

[5] Huang, S., Zhang, Z., Ke, T., Tang, M., & Xu, X. (2015). Scanning Photogrammetry for Measuring Large Targets in Close Range. *Remote Sensing*, 7, 10042–10077. https://doi.org/10.3390/rs70810042

[6] Ziobro, J. (2004). Efficiency of additional parameters in aerotriangulation. *Prace Instytutu Geodezji i Kartografii*, *L*(108), 145–154. (in Polish)

[7] Kacprzak, M. (2016). Application of GPS receivers and inertial measurement units to photo acquisition with use unmanned aerial vehicle (UAV). *Prace Instytutu Lotnictwa*, *3*(244), 267–276. https://doi.org/10.5604/05096669.1226159 (in Polish)

[8] Wierzbicki, D. (September, 2017). The prediction of position and orientation parameters of UAV for video imaging. In *The International Archives of the Photogrammetry, Remote Sensing and Spatial Information Sciences*, Germany, 407–413. https://doi.org/10.5194/isprs-archives-XLII-2-W6-407-2017

[9] Wierzbicki, D. (2018). Estimation of angle elements of exterior orientation for UAV images based on ins data and aerial triangulation processing. In *17th International Scientific Conference Engineering for Rural Development: proceedings* (pp. 1990–1996). https://doi.org/10.22616/ERDev2018.17.N054

[10] Jędryczka, R. (2000). Automation of the process of determining elements of external orientation. *Archiwum Fotogrametrii, Kartografii i Teledetekcji*, *10*, 44–1:44–9. (in Polish)

[11] Jędryczka, R. (2002). GPS/IMU measurements and determination of elements of external orientation. *Archiwum Fotogrametrii, Kartografii i Teledetekcji*, 12, 162–171. (in Polish)

[12] Wierzbicki, D., & Krasuski, K. (2020). Determining the Elements of Exterior Orientation in Aerial Triangulation Processing Using UAV Technology. *Communications – Scientific letters of the University of Zilina*, *22*(1), 15–24. https://doi.org/10.26552/com.C.2020.1.15-24

[13] Butowtt, J., & Kaczyński, R. (2010). *Photogrammetry*. Publishing House of the Military University of Technology. (in Polish)

[14] Hosseinpoor, H. R., Samadzadegan, F., & DadrasJavan, F. (2016). Pricise target geolocation and tracking based on UAV video imagery. *The International Archives of the Photogrammetry, Remote Sensing and Spatial Information Sciences*, *41*, 243–249. https://doi.org/10.5194/isprs-archives-XLI-B6-243-2016

[15] Santerre, R., Pan, L., Cai, C., & Zhu, J. (2014). Single Point Positioning Using GPS, GLONASS and BeiDou Satellites. *Positioning*, 5, 605, 107–114. https://doi.org/10.4236/pos.2014.54013

[16] Ashraf, S., Aggarwal, P., Damacharla, P., Wang, H., Javaid, A. Y., & Devabhaktuni, V. (2018). A low-cost solution for unmanned aerial 607 vehicle navigation in a global positioning system-denied environment. *International Journal of Distributed Sensor Networks*, 608, *14*(6), 1–17. https://doi.org/10.1177/1550147718781750

[17] Krasuski, K., Wierzbicki, D., & Bakuła, M. (2021). Improvement of UAV Positioning Performance Based on EGNOS+SDCM Solution. *Remote Sensing*, *13*(13), 2597. https://doi.org/10.3390/rs13132597

[18] Akpinar, B. (2021). Performance of UAV-Based Digital Orthophoto Generation for Emergency Response Applications. *TEM Journal*, *10*(4), 1721–1727. https://doi.org/10.18421/TEM104-31

[19] Szywalski, P., & Waindok, A. (2020). Practical Aspects of Design and Testing Unmanned Aerial Vehicles. *Acta Mechanica et Automatica*, *14*(1), 50–58. https://doi.org/10.2478/ama-2020-0008

[20] Hematulin, W., Kamsing, P., Torteeka, P., Somjit, T., Phisannupawong, T., & Jarawan T. (2023). Trajectory Planning for Multiple UAVs and Hierarchical Collision Avoidance Based on Nonlinear Kalman Filters. *Drones*, *7*, 142. https://doi.org/10.3390/drones7020142

[21] Li, K., Ma, H., & Wang, D. (September, 2021). Design of UAV navigation algorithm in single satellite environment based on high precision timing. In *32nd Congress of the International Council of the Aeronautical Sciences*, 6–11, China.

[22] Cisneros, I., Yin, P., Zhang, J., Choset, H., & Scherer, S. (2022). ALTO: A Large-Scale Dataset for UAV Visual Place Recognition and Localization. *The International Journal of Robotics Research*, *XX*(X). https://doi.org/10.48550/ARXIV.2207.12317

[23] Haddadi Amlashi, H., Samadzadegan, F., Dadrass Javan, F., & Savadkouhi, M. (2020). Comparing the accuracy of GNSS positioning variants for uav based 3D map generation. *The International Archives of the Photogrammetry, Remote Sensing and Spatial Information Sciences*, *43*, 443–449. https://doi.org/10.5194/isprs-archives-XLIII-B1-2020-443-2020

[24] Burdziakowski, P., & Bobkowska, K. (April, 2017). Accuracy of a low-cost autonomous hexacopter platforms navigation module for a photogrammetric and environmental measurements. *In 10th International Conference "Environmental Engineering"*, Lithuania. https://doi.org/10.3846/enviro.2017.173

[25] European GNSS Agency (GSA). (2020). *European Global Navigation Satellite Systems (EGNSS) for Drones Operations* [White paper]. https://doi.org/10.2878/52219

[26] Jimenez-Baños, D., Powe, M., Raj Matur, A., Toran, F., Flament, D., & Chatre, E. (September, 2011). EGNOS Open Service guidelines for receiver manufacturers. In Proceedings of the 24th International

*Metrol. Meas. Syst.*, Vol. 30 (2023), No. 3, pp. 441–459
DOI: 10.24425/mms.2023.146423

Technical Meeting of the Satellite Division of the Institute of Navigation (ION GNSS 2011) (pp. 2505–2512).

[27] Isik, O. K., Hong, J., Petrunin, I., & Tsourdos, A. (2020). Integrity Analysis for GPS-Based Navigation of UAVs in Urban Environment. *Robotics*, *9*(3), 66. https://doi.org/10.3390/robotics9030066

[28] Meng, L., Yang, L., Ren, S., Tang, G., Zhang, L., Yang, F., & Yang, W. (2021). An Approach of Linear Regression-Based UAV GPS Spoofing Detection. *Wireless Communications and Mobile Computing*, *2021*, 5517500. https://doi.org/10.1155/2021/5517500

[29] Basan, E., Makarevich, O., Lapina, M., & Mecella, M. (October, 2021). Analysis of the Impact of a GPS Spoofing Attack on a UAV. In *Proceedings of the International Workshop on Advanced in Information Security Management and Applications (AISMA 2021)* (pp. 6–16).

[30] Wei, X., Sun, C., Lyu, M., Song, Q., & Li, Y. (2022). CONSTDET: Control Semantics-Based Detection for GPS Spoofing Attacks on UAVs. *Remote Sensing*, *14*(21), 5587. https://doi.org/10.3390/rs14215587

[31] Grunwald, G., Ciećko, A., Kozakiewicz, T., & Krasuski, K. (2023). Analysis of GPS/EGNOS Positioning Quality Using Different Ionospheric Models in UAV Navigation. *Sensors*, *23*(3), 1112. https://doi.org/10.3390/s23031112

[32] Pochwała, S., Gardecki, A., Lewandowski, P., Somogyi, V., & Anweiler, S. (2020). Developing of Low-Cost Air Pollution Sensor – Measurements with the Unmanned Aerial Vehicles in Poland. *Sensors*, *20*(12), 3582. https://doi.org/10.3390/s20123582

[33] Ahmed, S., El-Shazly, A., Abed, F., & Ahmed, W. (2020). The Influence of Flight Direction and Camera Orientation on the Quality Products of UAV-Based SfM-Photogrammetry. *Applied Sciences*, *12*(20), 10492. https://doi.org/10.3390/app122010492

[34] Zhao, X., Pu, F., Wang, Z., Chen, H., & Xu, Z. (2019). Detection, Tracking, and Geolocation of Moving Vehicle from UAV Using Monocular Camera. *IEEE Access*, 7, 101160–101170. https://doi.org/10.1109/ACCESS.2019.2929760

[35] Elsheshtawy, A. M., & Gavrilova, L. A. (2021). Improving Linear Projects Georeferencing to Create Digital Models Using UAV Imagery. In *E3S Web of Conferences* (Vol. 310, p. 04001). EDP Sciences. https://doi.org/10.1051/e3sconf/202131004001

[36] Forlani, G., Diotri, F., Morra di Cella, U., & Roncella, R. (2020). UAV Block Georeferencing and Control by On-Board GNSS Data. *The International Archives of the Photogrammetry, Remote Sensing and Spatial Information Sciences*. XLIII-B2-2020, 9–16. https://doi.org/10.5194/isprs-archives-XLIII-B2-2020-9-2020

[37] Zhang, H., Aldana-Jague, E., Clapuyt, F., Wilken, F., Vanacker, V., & Van Oost, K. (2019). Evaluating the potential of post-processing kinematic (PPK) georeferencing for UAV-based structure-from-motion (SfM) photogrammetry and surface change detection. *Earth Surface Dynamics*, *7*(3), 807–827. https://doi.org/10.5194/esurf-7-807-2019

[38] Chiang, K. W., Tsai, M. L., & Chu, C. H. (2012). The development of an UAV borne direct georeferenced photogrammetric platform for ground control point free applications. *Sensors*, *12*(7), 9161–9180. https://doi.org/10.3390/s120709161

[39] Sanyal, S., Bhushan, S., & Sivayazi, K. (2020, January). Detection and location estimation of object in unmanned aerial vehicle using single camera and GPS. In *2020 First International Conference on Power, Control and Computing Technologies (ICPC2T)* (pp. 73–78). IEEE. https://doi.org/10.1109/ICPC2T48082.2020.9071439

[40] Sun, H., Li, L., Ding, X., & Guo, B. (2016). The precise multimode GNSS positioning for UAV and its application in large scale photogrammetry. *Geo-spatial Information Science*, *19*(3), 188–194. https://doi.org/10.1080/10095020.2016.1234705

[41] Grenzdörffer, G. J., Engel, A., & Teichert, B. (2008). The photogrammetric potential of low-cost UAVs in forestry and agriculture. *The International Archives of the Photogrammetry, Remote Sensing and Spatial Information Sciences*, *31*(B3), 1207-1214.

[42] Diep, J., Gómez-Casco, D., Villamide, X. O., Swinden, R. D., & Crosta, P. (2022, April). Performance Analysis of Mass-Market GNSS Receivers in UAV Applications. In *2022 10th Workshop on Satellite Navigation Technology (NAVITEC)* (pp. 1–8). IEEE. https://doi.org/10.1109/NAVITEC53682.2022.9847551

[43] Noviello, C., Esposito, G., Fasano, G., Renga, A., Soldovieri, F., & Catapano, I. (2020). Small-UAV radar imaging system performance with GPS and CDGPS based motion compensation. *Remote Sensing*, *12*(20), 3463. https://doi.org/10.3390/rs12203463

[44] Elamin, A., Abdelaziz, N., & El-Rabbany, A. (2022). A GNSS/INS/LiDAR Integration Scheme for UAV-Based Navigation in GNSS-Challenging Environments. *Sensors*, *22*(24), 9908. https://doi.org/10.3390/s22249908

[45] Schaer, S. (1999). *Mapping and predicting the Earth's ionosphere using Global Positioning System* [Doctoral dissertation, University of Berne].

[46] Le, A. Q., & Tiberius, C. (2007). Single-frequency precise point positioning with optimal filtering. *GPS Solutions*, *11*(1), 61–69. https://doi.org/10.1007/s10291-006-0033-9

[47] Krasuski, K. (2019). *The research of accuracy of aircraft position using SPP code method* [Doctoral dissertation, Warsaw University of Technology] (in Polish)

[48] Nie, Z., Zhou, P., Liu, F., Wang, Z., & Gao, Y. (2019). Evaluation of orbit, clock and ionospheric corrections from five currently available SBAS L1 services: methodology and analysis. *Remote Sensing*, *11*(4), 411. https://doi.org/10.3390/rs11040411

[49] Molina, P., Colomina, I., Vitoria, T., Freire, P., Skaloud, J., Kornus, W., Mata, R., & Aguilera, C. (May, 2011). The CLOSE-SEARCH project UAV-based search operations using thermal imaging and EGNOS-SoL navigation. In *Proceedings of the GeoInformation for Disaster Management Conference* (Gi4DM 2011), Antalya, Turkey, 3–7.

[50] Wierzbicki, D., & Krasuski, K. (2016). Determination the coordinates of the projection center in the digital aerial triangulation using data from Unmanned Aerial Vehicle. *Aparatura Badawcza i Dydaktyczna*, *2016*(3), 127–134. (in Polish)

[51] Wierzbicki, D., & Krasuski, K. (2016). The correction methods of heading, pitch, roll rotation angles with using UAV. *Modelowanie Inżynierskie*, *27*(58), 132–138. (in Polish)

[52] Osada, E. (2001). *Geodesy*. Oficyna Wydawnicza Politechniki Wrocławskiej. (in Polish)

[53] CODE LAC Website. (2023). http://ftp.aiub.unibe.ch/CODE/

[54] Takasu, T. (2013). RTKLIB ver. 2.4.2 Manual, RTKLIB: An Open Source Program. Package for GNSS Positioning. http://www.rtklib.com/prog/manual_2.4.2.pdf

[55] Specht, M., Specht, C., Stateczny, A., Burdziakowski, P., Dąbrowski, P., & Lewicka, O. (2022). Study on the Positioning Accuracy of the GNSS/INS System Supported by the RTK Receiver for Railway Measurements. *Energies*, *15*, 4094. https://doi.org/10.3390/en15114094

[56] MAGNET Tools Website. (2023). https://www.topconpositioning.com/office-software-and-services/survey-software/magnet-tools

[57] Scilab Website. (2023). https://www.scilab.org/

[58] Scibbr Website, (2023). https://www.scribbr.com/statistics/coefficient-of-determination

*Metrol. Meas. Syst.*, Vol. 30 (2023), No. 3, pp. 441–459
DOI: 10.24425/mms.2023.146423

[59] Tabti, L., Kahlouche, S., Benadda, B., & Beldjilali, B. (2020). Improvement of single-frequency GPS positioning performance based on EGNOS corrections in Algeria. *The Journal of Navigation*, *73*(4), 846–860. https://doi.org/10.1017/S037346331900095X

**Kamil Krasuski** received the Ph.D. degree from Warsaw University of Technology, Poland, in 2019. He is currently an Assistant Professor in the Institute of Navigation in the Polish Air Force University in Dęblin. He has authored or coauthored 1 book, 30 book chapters, over 100 journal and 15 conference publications. His current research interests include implementation GNSS satellite systems in aviation.

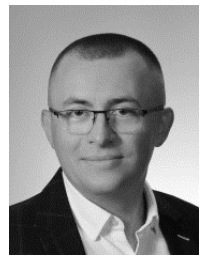

**Damian Wierzbicki** received the Ph.D. degree in photogrammetry and remote sensing from the Military University of Technology, Warsaw, Poland in 2015. He is currently an Associate Professor with the Department of Imagery Intelligence, Faculty of Civil Engineering and Geodesy, Military University of Technology where he teaches: "Photogrammetry and Remote Sensing" and "Image Processing". His research interests include UAV navigation and image processing, deep learning in remote sensing. His research interests also include development of new algorithms for object detection and classification in image sequences from UAVs.

**Marta Lalak** received the M.Sc. degree in geoinformatics from the Military University of Technology, Warsaw, Poland in 2010. Currently she is working towards a Ph.D. in engineering and technical sciences. She is a lecturer at the Institute of Navigation of the Polish Air Force University, where she conducts classes on "GIS in Navigation", "Basics of Photogrammetry", "Basics of Remote Sensing", "Image recognition". Her research interests include UAV-acquired data processing and aviation obstacle detection.

**Adam Ciećko** received the Ph.D. degree from the University of Warmia and Mazury (UMW) in Olsztyn, Poland in 2002 in the field of geodesy and cartography. He is currently an Associate Professor and member of the scientific staff at the Institute of Geodesy and Civil Engineering, UWM Olsztyn. He has been involved in many projects related to GNSS kinematic positioning of aircraft and moving land vehicles. He has extensive experience in the use of GNSS technology in navigation. Since 2004, he has been involved in the process of validation and certification of GNSS receivers in accordance with EU regulations.